STEADY VISCOUS FLOW PAST A CIRCULAR CYLINDER

BENGT FORNBERG

DEPARTMENT OF APPLIED MATHEMATICS
CALIFORNIA INSTITUTE OF TECHNOLOGY

PASADENA, CALIFORNIA

STEADY VISCOUS FLOW PAST A CIRCULAR CYLINDER

Bengt Fornberg
Department of Applied Mathematics 217-50
California Institute of Technology
Pasadena, Ca 91125.

ABSTRACT

Viscous flow past a circular cylinder becomes unstable around Reynolds number Re = 40. With a numerical technique based on Newton's method and made possible by the use of a supercomputer, steady (but unstable) solutions have been calculated up to Re = 400. It is found that the wake continues to grow in length approximately linearly with Re. However, in conflict with available asymptotic predictions, the width starts to increase very rapidly around Re = 300. All numerical calculations have been performed on the CDC Cyber 205 at the CDC Service Center in Arden Hills, Minnesota.

INTRODUCTION

The structure of viscous steady flow past a circular cylinder at high Reynolds numbers forms one of the classical problems in fluid mechanics. In spite of much attention, several fundamental questions remain open. Apart from a previous calculation by the present author [6], complete, steady flow fields have been obtained numerically only up to around Re = 100. This is also close to the upper limit for experiments (due to temporal instabilities). Both the early numerics and the experiments point to a recirculation region growing linearly in length with Re. Figure 1 shows the length of the wake bubble against Reynolds number according to some different calculations. Persistence of this growth for Re -> ∞ has been assumed in most

recent asymptotic studies of steady high Reynolds number flows past a body (e.g. F.T. Smith [13]). A possible Euler flow, consistent with this idea, was analyzed by Brodetsky [3] in 1923. It is known as the Helmholtz- Kirchhoff free streamline model. This suggested limit is characterized by two vortex sheets leaving the body tangentially approximately 55° from the upwind center line and extending to downstream infinity, enclosing a region of stagnant flow. Although this undoubtedly is a solution for Re = ∞, G.K. Batchelor [2] gave in 1956 several arguments against this being a possible limit for Re -> ∞. He proposed an alternative in which a finite wake with piecewise constant vorticity was bounded by vortex sheets. Some suggestions about how such a flow might be reached as a limit for increasing Reynolds number have been given by Peregrine [10]. However, only very few Euler solutions of this so called Prandtl-Batchelor type have been calculated (e.g.[12] contains one example and some further references). None of these are for flow past a cylinder. Figure 2 gives an 'artists impression' of what the two models for infinite Re might look like. The calculation [6] hinted at a process leading to a shortening of the wake. The present work suggests (in agreement with F.T. Smith [14]) this shortening at Re = 300 was erroneous and caused by insufficient numerical resolution. However, our best current evidence is that the qualitative result was correct. We beleive that a reversal of trends towards a shorter wake can be expected around Re = 500. This contrasts with the conclusions in [14]. Our main evidence is that the wake increases in width far more rapidly after Re = 300 than the asymtotic analysis allows for. Independently of the position of artificial boundaries and of numerical resolution, we find that the flow is of different character past Re = 300. Significant amounts of vorticity are then re-circulated back into the wake bubble from its end. We hope to soon carry this study past Re = 400.

MATHEMATICAL FORMULATION.

With a cylinder of radius 1 and a Reynolds number based on the diameter, the governing time independent Navier-Stokes equations, expressed in streamfunction Ψ and vorticity ω , take the form:

$$(1) \quad \Delta\Psi + \omega = 0$$

$$(2) \quad \Delta\omega + \frac{Re}{2}\left\{\frac{\partial\Psi}{\partial x}\cdot\frac{\partial\omega}{\partial y} - \frac{\partial\Psi}{\partial y}\cdot\frac{\partial\omega}{\partial x}\right\} = 0$$

Accurate numerical approximation and economical computational solution of these equations in the given geometry poses a series of difficulties which previous investigators have dealt with in a variety of ways. The most serious of the difficulties seem to be:

1. Boundary comditions for Ψ at large distances.

2. Boundary condition for ω at the body surface.

3. Avoiding the loss of accuracy that comes with upwind differencing.

4. Economical choice of computational grid.

5. Reliable and fast rate of convergence of numerical iterations.

The point 5 above has been the limiting factor in virtually all previous attempts to reach high Reynolds numbers. No reliable technique has emerged to prevent slowly converging iteration schemes from picking up physical instabilities in the artificial time of the iterations.

NUMERICAL METHOD

All vorticity is concentrated on the body surface and in a quite thin wake downstream of the body. Outside this region we can use the much simpler equations:

(3) $$\Delta \Psi = 0$$

(4) $$\omega = 0$$

The top part of Figure 3 shows the upper half plane minus a unit circle and, dotted, a region which contains all the vorticity (apart from the far wake). The bottom part of the figure shows how the mapping $z = \sqrt{x} + 1/\sqrt{x}$ maps these to the first quadrant and a rectangle respectively. Figure 4 shows what a rectangular grid in the z-plane (with non-uniform stretching in the vertical direction) can look like in the x-plane. The Navier-Stokes equations, transformed to the z-plane take a form almost identical to (1) and (2):

(5) $$\Delta \Psi + \omega/J = 0$$

(6) $$\Delta \omega + \frac{Re}{2} \left\{ \frac{\partial \Psi}{\partial \xi} \cdot \frac{\partial \omega}{\partial \eta} - \frac{\partial \Psi}{\partial \eta} \cdot \frac{\partial \omega}{\partial \xi} \right\} = 0$$

where $J = \left| \frac{dz}{dx} \right|^2$ is the Jacobian of the mapping. These equations were modified further by subtracting out potential flow. The stream function for the difference is $\Psi = \Psi - 2\xi\eta$. On a grid in the (stretched) z-plane, equations (5) and (6) were approximated at all interior points with centered second order finite differences. To close the system, boundary conditions have to be implemented for Ψ and ω at all boundaries.

The extreme sensitivity of the final solution to small errors in these conditions has only recently been fully recognized [6]. For example already at Re = 2 it was found that use of the free stram value for Ψ along circular outer boundaries at distances 23.1 and 91.5 caused 18 % and 4.4 % errors in the level of vorticity on the body surface.

The 'Oseen' approximation is the leading term in an asymptotic expansion for the flow far out in a wake (e.g. Imai [8]). In polar coordinates, it takes the form

$$(7) \qquad \psi = \frac{C_D}{2} \left(\frac{\theta}{\pi} - \text{erf } Q \right)$$

$$(8) \qquad \omega = - \frac{C_D \, \text{Re} \, Q}{4 \, \sqrt{\pi} \, r} \, e^{-Q^2}$$

where $Q = \left(\frac{1}{2} \text{Re } r \right)^{1/2} \sin \frac{1}{2} \theta$, $\text{erf } Q = 2\pi^{-1/2} \int_0^Q e^{-s^2} ds$ and C_D the drag coefficient. C_D can be evaluated as a line integral around the body.

The performance of this Oseen condition as an outer boundary condition is disappointing. The percentage errors mentioned above improve, but only to to 3.4 % and 1.2 % respectively. For increasing Re, direct use of (7) becomes meaningless. Figure 5 illustrates this by comparing the true ψ (here the difference between streamfunction and free stream, not potential flow) with the values from (7) at Re = 200. The two fields bear no resemblance to each other at the distances from the body we are interested in.

Comparison with numerics suggest that (8) is far more accurate than (7). Furthermore

1. Any errors in (8) are present only in a very narrow region along the outflow axis, not along the whole upper boundary as with (7).

2. The governing equation for ω is of a type which cannot transport incorrect information for ω back up towards the cylinder.

With this background, let us briefly outline how the boundary conditions of high accuracy can be implemented on the edges of the present computational region. Figure 6 shows this region in the z-plane with a typical vorticity field together with its reflections in the coordinate axis.

205

BOUNDARY CONDITIONS FOR Ψ.

Left boundary: $\xi = 0$, $0 \leq \eta \leq \eta_N$. $\qquad \Psi = 0$.

Bottom boundary: $\eta = 0$, $0 \leq \xi \leq \xi_M$. $\qquad \Psi = 0$.

Right boundary: $\xi = \xi_M$, $0 \leq \eta \leq \eta_N$. $\qquad \dfrac{\partial^2 \Psi}{\partial \eta^2} = \omega$ (noting that $\dfrac{\partial^2 \Psi}{\partial \xi^2} \ll$

$$\ll \dfrac{\partial^2 \Psi}{\partial \eta^2} \text{ along this boundary}).$$

Top boundary: $\eta = \eta_N$, $0 \leq \xi \leq \xi_M$. $\qquad \Psi_{\xi,\eta_N} = \displaystyle\int_{-\xi_M}^{\xi_M} \int_{-\eta_N}^{\eta_N} \omega \ln((\xi_c-\xi)^2 + (\eta_c-\eta)^2)/J \; d\xi d\eta$

A correction to the integral above for vorticity reaching outside the downstream boundary can easily be incorporated. For a fixed grid, the dependence of Ψ at each boundary point on ω at each internal point is independent of Re and can be calculated as a large matrix once and for all. A boundary condition of this kind was used in all the calculations presented below. However, we currently use a different condition. A wide two level difference formula can be found which is consistent only with the decaying modes of the equation $\Delta \Psi = 0$ (as opposed to the usual 5-point 3-level formula used inside the region to approximate both growing and decaying modes).

BOUNDARY CONDITIONS FOR ω.

Left boundary: $\xi = 0$, $0 \leq \eta \leq \eta_N$. $\qquad \omega = 0$.

Bottom boundary: $\eta = 0$, $0 \leq \xi < 2$. $\qquad$ A relation based on $\Delta \Psi + \omega/J = 0$
and Ψ an even function of η .

$\qquad\qquad\qquad\qquad 2 \leq \xi \leq \xi_M$. $\qquad \omega = 0$.

Right boundary: $\xi = \xi_M$, $0 \leq \eta \leq \eta_N$. $\qquad \omega_{\xi_M} = \omega_{\xi_{M-1}}(\xi_M/\xi_{M-1})^2$

Top boundary: $\eta = \eta_N$, $0 \leq \xi \leq \xi_M$. $\qquad \omega = 0$.

The condition at the right boundary comes from the observation that the leading term of (8), transformed to ξ, η -coordinates simplifies to

(9) $\qquad \omega = \dfrac{c_1}{\xi^2} \eta \, e^{-c_2 \eta}$

where c_1 and c_2 are constants. The mapping has achieved a separation of variables.

The discrete approximations at the interior points together with the boundary conditions form, after minor simplifications (explicitly eliminating all boundary unknowns apart from Ψ at the top boundary), a non-linear algebraic system of (M-2)(2N-3) equations with equally many unknowns. In most earlier works, great care has been taken to ensure that, at this stage, this (or some equivalent) non-linear system has a diagonally dominant form for low Re. This would allow direct functional iteration to convergence. Techniques like upwind differencing [1],[4],[11] help in this respect at the cost of lowered accuracy. Newton's method, described below, offers an outstanding alternative.

NEWTON'S METHOD.

Newton's method is a very well known procedure for finding zeros of scalar functions. If a function $f(x)$ is given, we can find an x such that $f(x)=0$ by the procedure:

(10) x_0 'close' guess of root

(11) $$x_{n+1} = x_n - \frac{f(x_n)}{f'(x_n)} \qquad n = 0, 1, 2, \ldots$$

The iteration step can be written

(12) $$f'(x_n) \, \Delta x_n = -f(x_n)$$

Known, f' evalu-   Unknown, the   Known, residual.
ated at the latest correction we   Should be zero
available approxi- should apply   if x_n had been
mation x_n.   to x_n, i.e. exact.
                    $x_{n+1} = x_n + \Delta x_n$.

Written in this form, the generalization to systems is straightforward. For example the system with three equations in three unknowns:

207

$$(13) \qquad \begin{aligned} f(x,\ y,\ z) &= 0 \\ g(x,\ y,\ z) &= 0 \\ h(x,\ y,\ z) &= 0 \end{aligned}$$

can be iterated

$$
\begin{bmatrix}
\dfrac{\partial f}{\partial x} & \dfrac{\partial f}{\partial y} & \dfrac{\partial f}{\partial z} \\[1em]
\dfrac{\partial g}{\partial x} & \dfrac{\partial g}{\partial y} & \dfrac{\partial g}{\partial z} \\[1em]
\dfrac{\partial h}{\partial x} & \dfrac{\partial h}{\partial y} & \dfrac{\partial h}{\partial z}
\end{bmatrix}
\begin{bmatrix} \Delta x \\[1em] \Delta y \\[1em] \Delta z \end{bmatrix}
= -
\begin{bmatrix} f(x,y,z) \\[1em] g(x,y,z) \\[1em] h(x,y,z) \end{bmatrix}
$$

Known, "Jacobian"   Unknown,   Known,
of system.   corrections.   residual.

Each iteration involves the solution of a linear system. Like in the scalar case, convergence is quadratic and guaranteed to occur for approximations sufficiently close to any 'simple' solution. The realization that this procedure is practical for extremely large systems (several thousands of equations) is rather recent and linked to the emergence of powerful computers.

For our present problem, use of Newton's method offers several major advantages:

1. The quadratic convergence allows no possibility of 'inheriting' temporal instabilities to the artificial time of the iterations. Convergence is guaranteed if an isolated solution exists in the neighborhood of a guess.

2. If turning points or bifurcation points are found, they will cause no difficulties.

3. No upwind differencing is needed. This procedure is typically employed for two reasons:

1. To ensure convergence of an iterative method.

2. To avoid mesh size oscillations.

The first reason no longer applies. The second one alone can
then be addressed in more refined ways.

4. Boundary conditions at the body surface become easier to
    implement. The fact that we have two conditions on Ψ and none
    on ω can cause a problem if (5) and (6) are treated separately.
    With Newton's method, all we need is that the number of
    conditions is right.

The only disadvantage with Newton's method is the computational
cost. This is where supercomputers enters our picture.

SOLUTION OF LINEAR SYSTEM

Let $[\Psi]_j$, j=2,3,...,N be vectors with Ψ -values from grid lines
2,3,...,N and similarly for ω_j (j=2,...,N-1). For example Ψ_2 would
contain the Ψ -values along the grid row nearest to the ξ -axis and
Ψ_N the values along the top boundary. The structure of the entries in
the Jacobian matrix reflects directly on the difference stencils and
the boundary conditions. Figure 7 shows a suitable ordering of
equations and unknowns and the corresponding structure of the
Jacobian. Since the top right corner contains a single diagonal,
explicit multiples of the top (N-2)(M-2) equations can be superposed
on the equations below to modify the structure to the one in Figure
8. The bottom left corner form a separated system of size (N-1)(M-2).
This system was solved by a border algorithm similar to the one
described in [9]. The major cost comes from the LU-factorization of
A. However, one more rearrangement can be done to achieve a
significant speedup. The A-matrix has a block 5-diagonal form with
the structure shown in Figure 8. A similarity transform with a
permutation matrix can rearrange this into another matrix of
identical structure. Instead of N-2 rows of blocks, each of size M-2,
we get M-2 rows of blocks of size N-2. With M typically around 6*N
and cost proportional to the square of the bandwidth, this reduces
the memory needed for the LU-decomposition about 6 and the operation
count by 36.

The complete linear solver lends itself ideally to
vectorization. Every part of significant cost turns out take a form
of a 'linked triad' with vectors never shorter than 4(N-2)+1 or M.
The linked triad on the Cyber 205 is the fastest floating point

operation the machine offers. Expressions of the form vector-op-vector-op-scalar where one 'op' is + or -, the other * can execute with both operations running simultaneously. On the 2-pipe 205, the algorithm has a potential for 200 mflops (million floating point operations per second, 64-bit accuracy). Including a startup cost of 83 macihne cycles per linked triad operation, average vector length of around 166 (which we will exceed in later test cases) could give a full 100 mflop overall computational performance. In the calculations presented below, the grid had 131 by 21 points. Building up the Jacobian (in scalar mode) takes 2.3 seconds and the solution of the linear system 3.7 seconds (for an average of 55 mflops during this part). Recently implemented vectorization of the Jacobian and the new boundary condition brings these numbers to 0.026 seconds, 1.75 seconds and 60 mflops respectively.

PHYSICAL CONCLUSIONS

This report is a preliminary one of work in progress. Only a few initial test runs have been performed so far. However, we can already conclude that the wake appears to continue a linear growth in length with increasing Reynolds numbers up to Re = 400. Figure 9 shows wake length versus Re for some previous calculations compared with current results. Figure 10 shows streamlines and Figure 11 vorticity fields for different values of Re up to 400. The vorticity field at Re = 400 shows a recirculation back into the wake from the end of the bubble as well as a quite sudden increase in width. Our most recent tests with a computational grid of 196 by 31 points (density increased by 3/2 in each direction) leaves these features completely unchanged. The onset occurs near Re = 300 and the widening progresses at a rate which can be determined accurately and which far exceeds the one predicted by available asymptotic models.

The flow fields in figures 10 and 11 were obtained from a 131*21 grid in the z-plane with

(14) $\xi_i = i/12$, i=0,1, ... ,130

(15) $\eta_j = \kappa \zeta_j^3 + (1-4\alpha)\zeta_j$, $\zeta_j = j/18$, j=0,1, ... ,20 , $\kappa = 0.15$

This places the right boundary at a distance 115.4 from the center of the cylinder.   Preliminary tests involving moving this and the top boundaries in and out suggest that they are sufficiently far out with the present choice of grid. Figure 4 showed part of this grid.

The major open questions at the moment are:

Physically:

1.   Will the wake keep on growing?

2.   Are there any other branches of solutions (bifurcations etc.)?

Numerically:

1.   Is there any alternative to Newton's method which still possesses a reliable rate of convergence?

2.   Is there any faster way than Gaussian elimination to solve the linear system in Newton's method?

At present, the numerical questions are wide open and of fundamental importance to many other applications as well. Current numerical methods together with vector computers like the Cyber 205 probably form sufficiently powerful tools to settle conclusively the physical questions raised here.
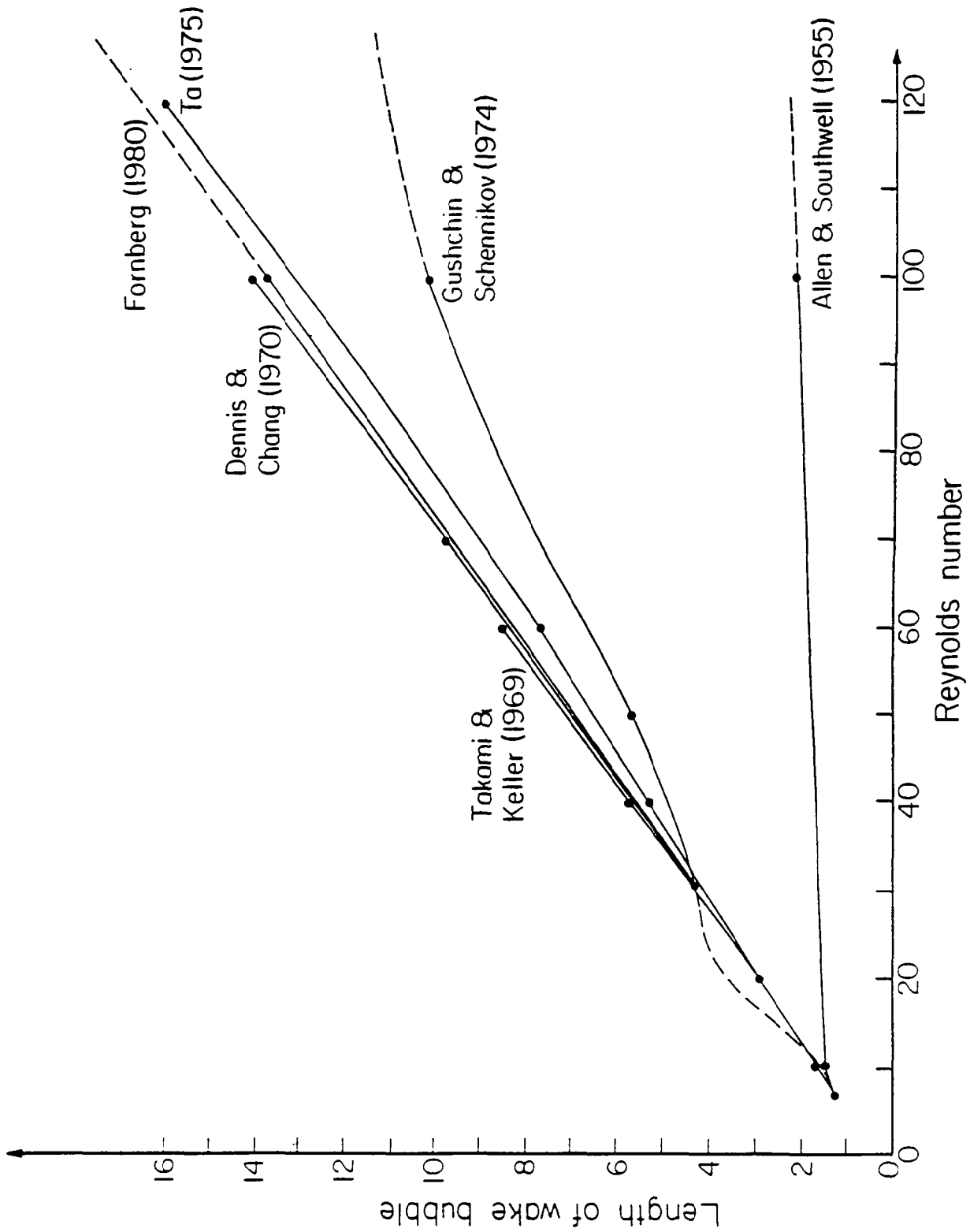
Figure 1. Length of wake bubble for low Reynolds numbers according to some different calculations.

Figure 2. Schematic illustration of free streamline and
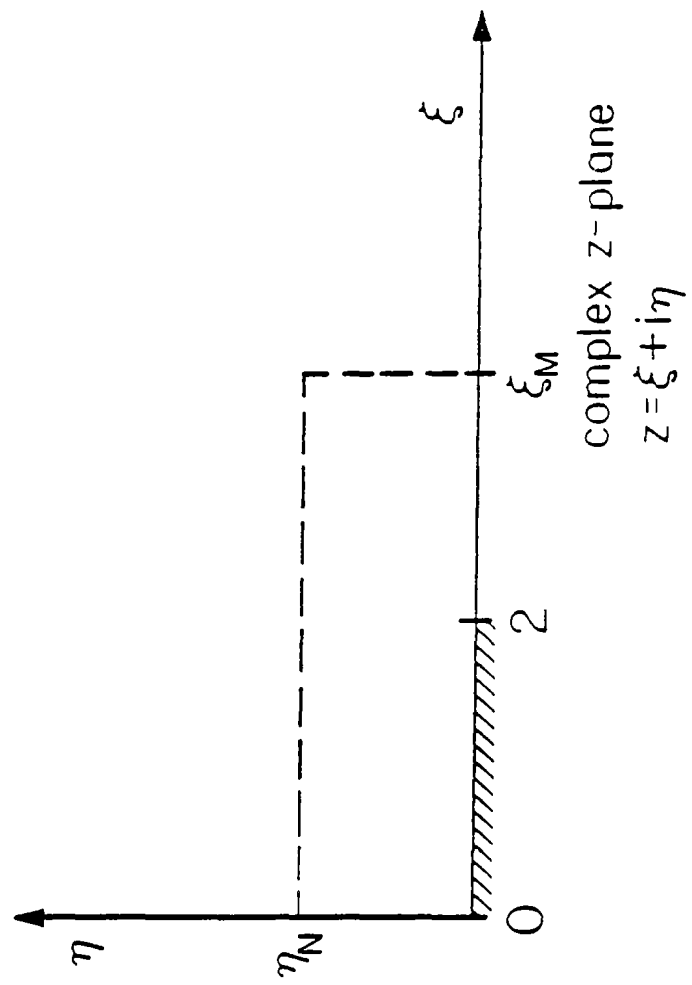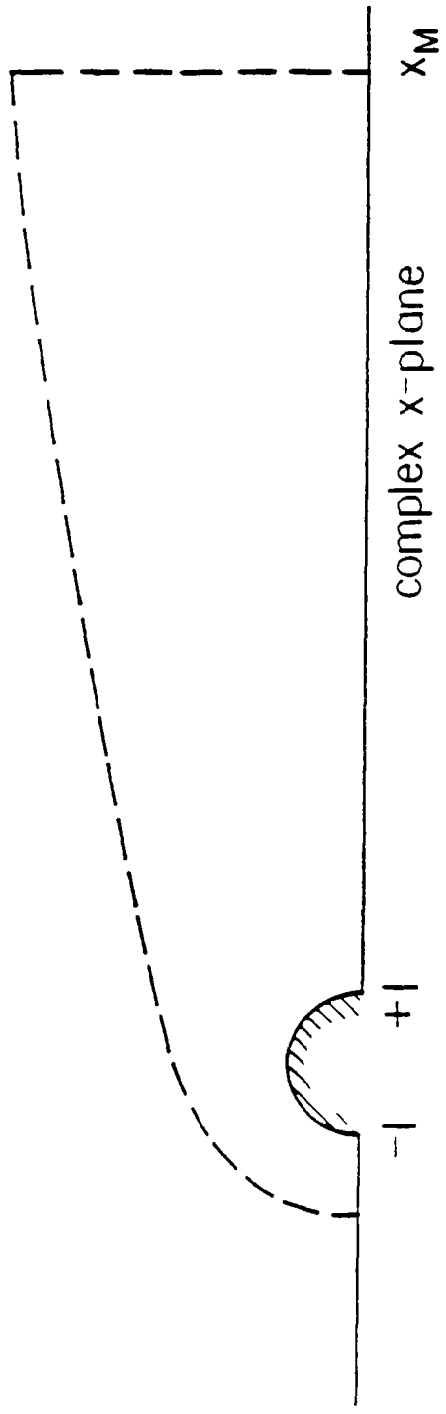the Prandtl-Batchelor models.

213

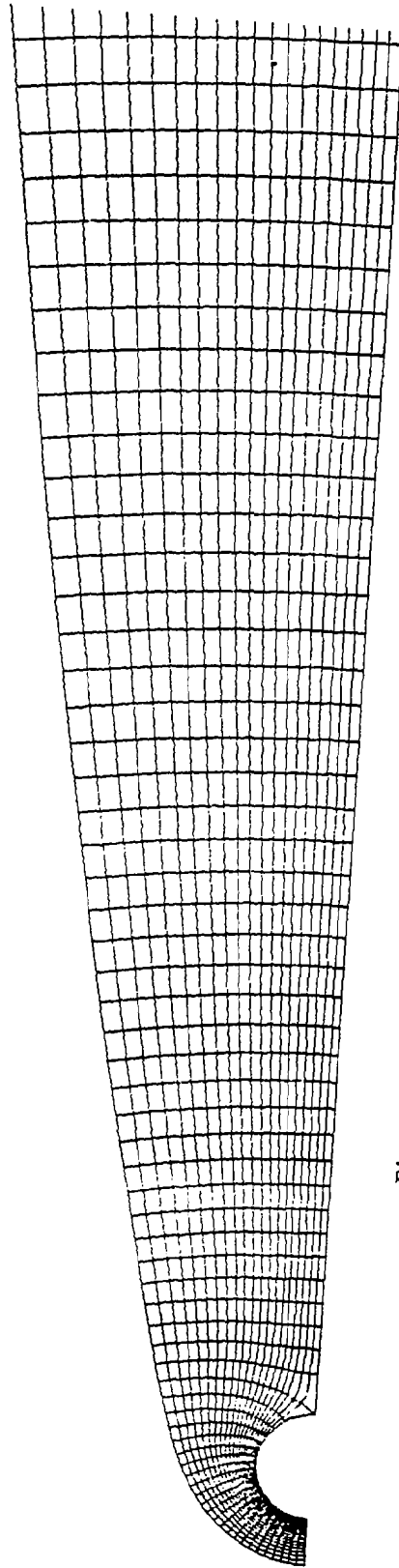Figure 3. Conformal mapping of computational region.

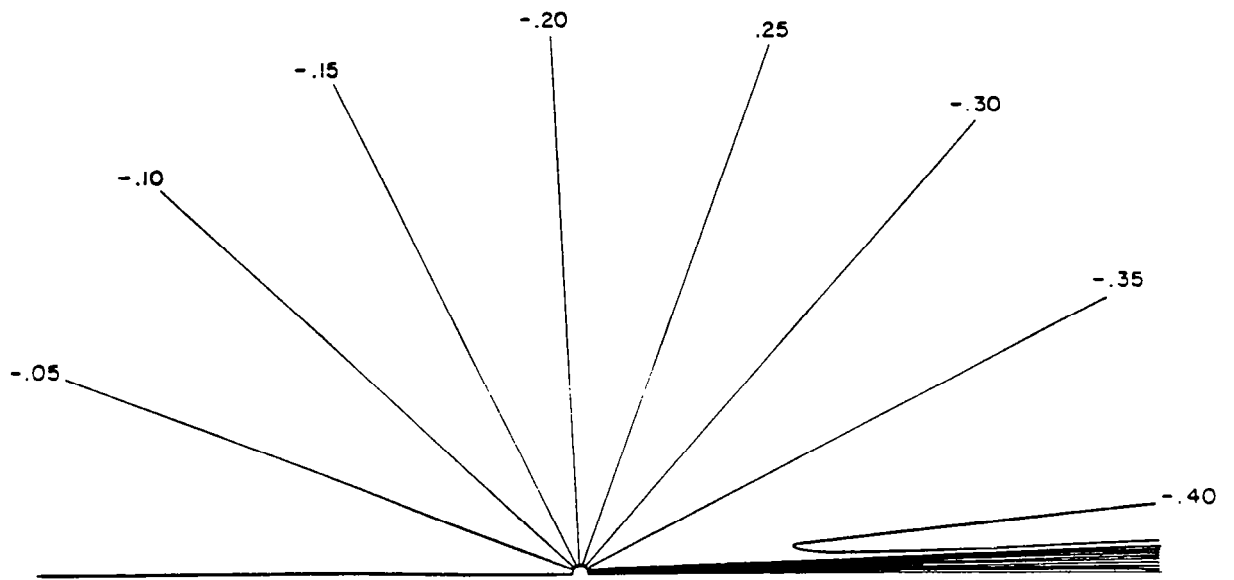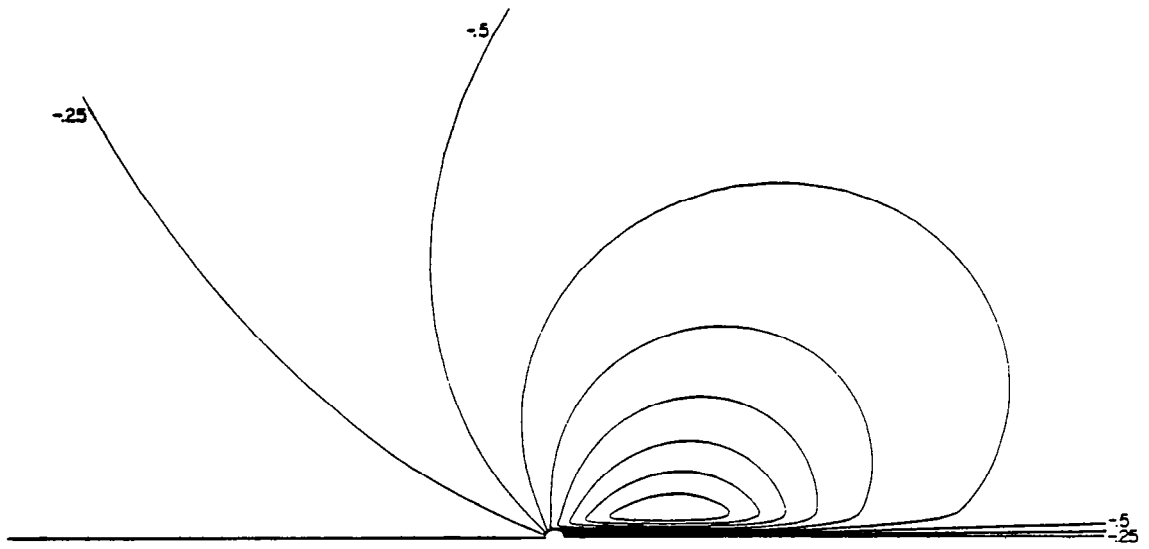Figure 4.   Part near cylinder of computational grid.

215

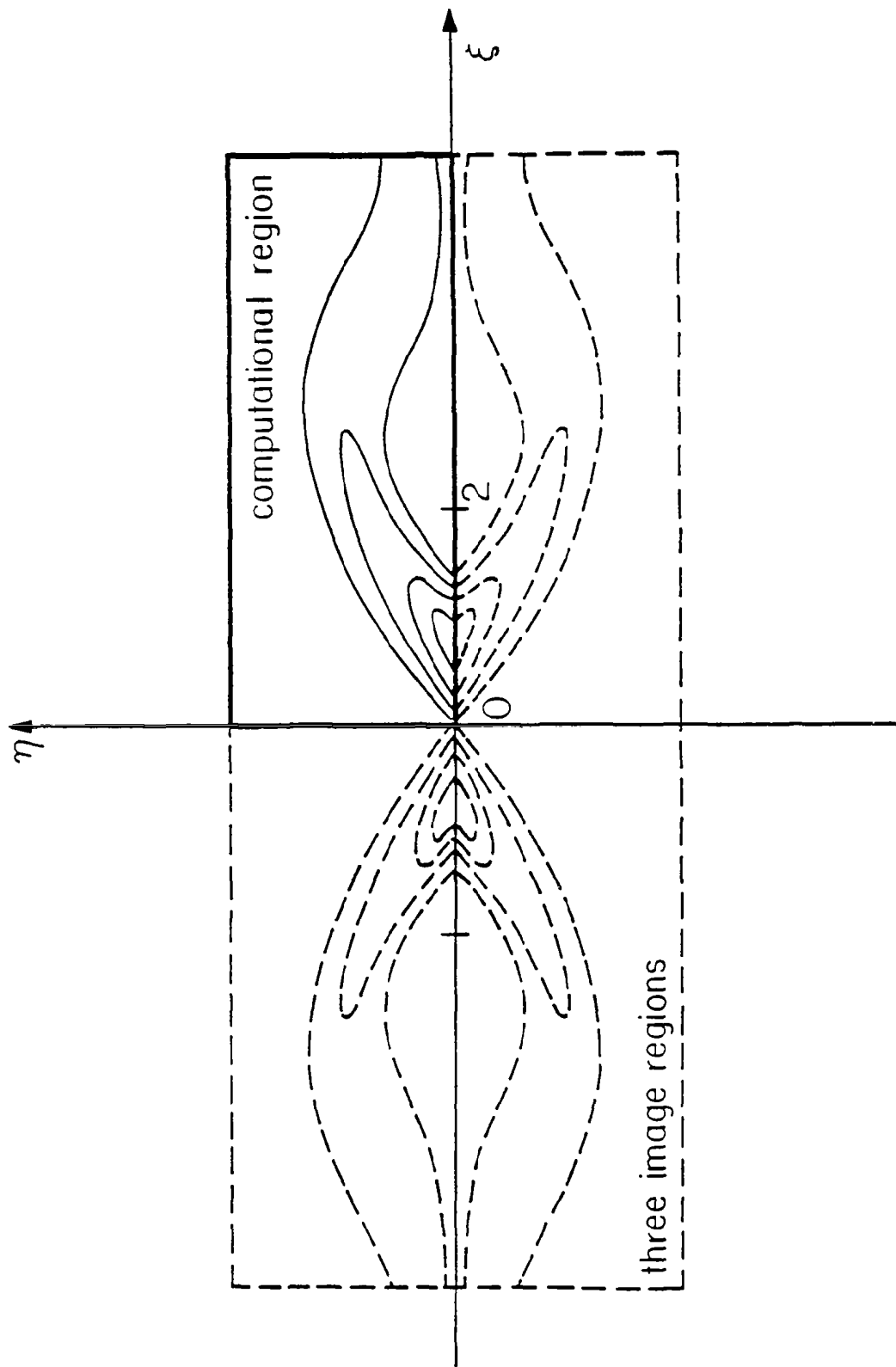Figure 5. True difference between streamfunction and free stream compared with Oseen approximation for Re = 200.
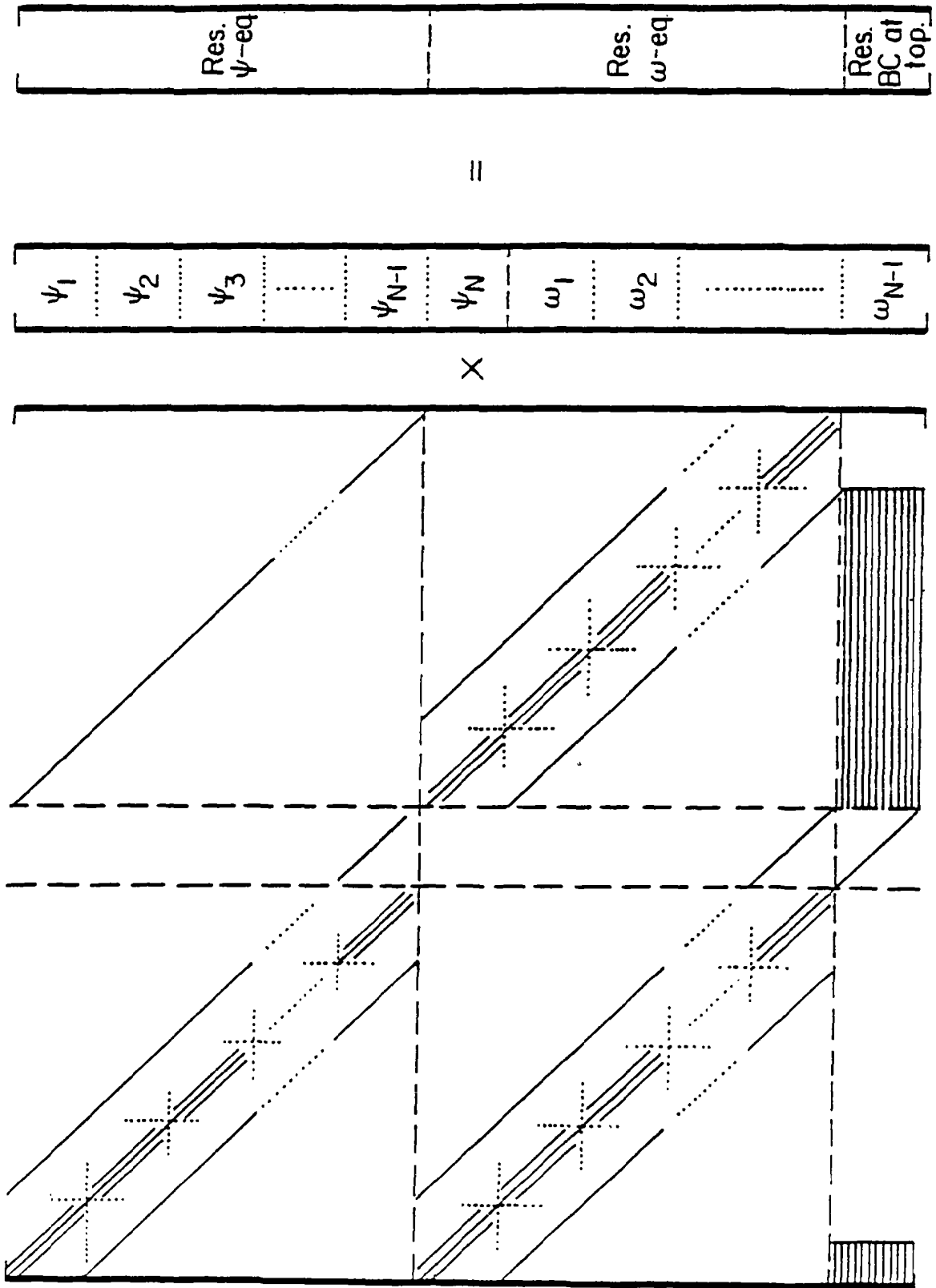
Figure 6. Typical vorticity field in complex z-plane.
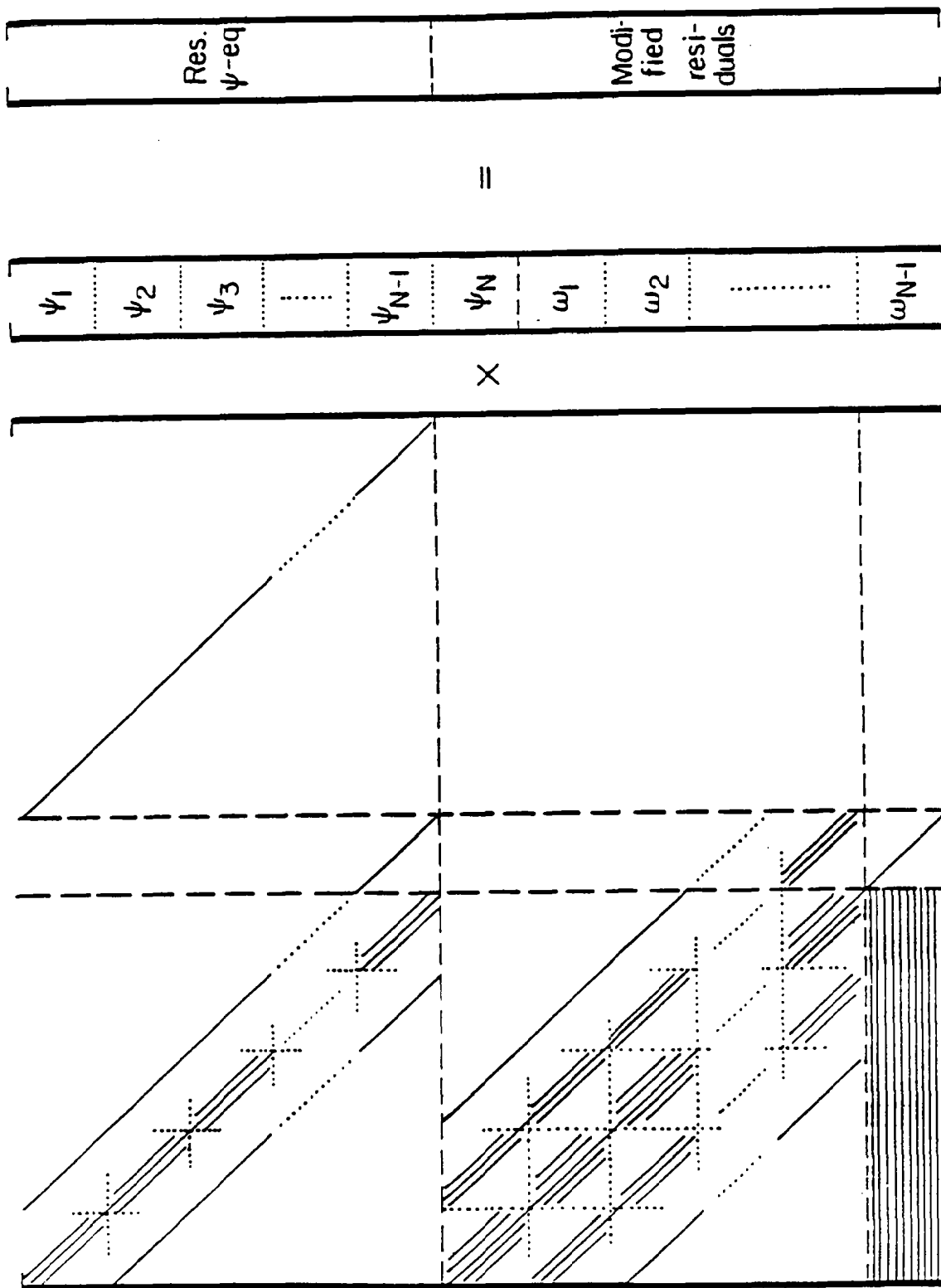
Figure 7. Linear system in Newton's method.

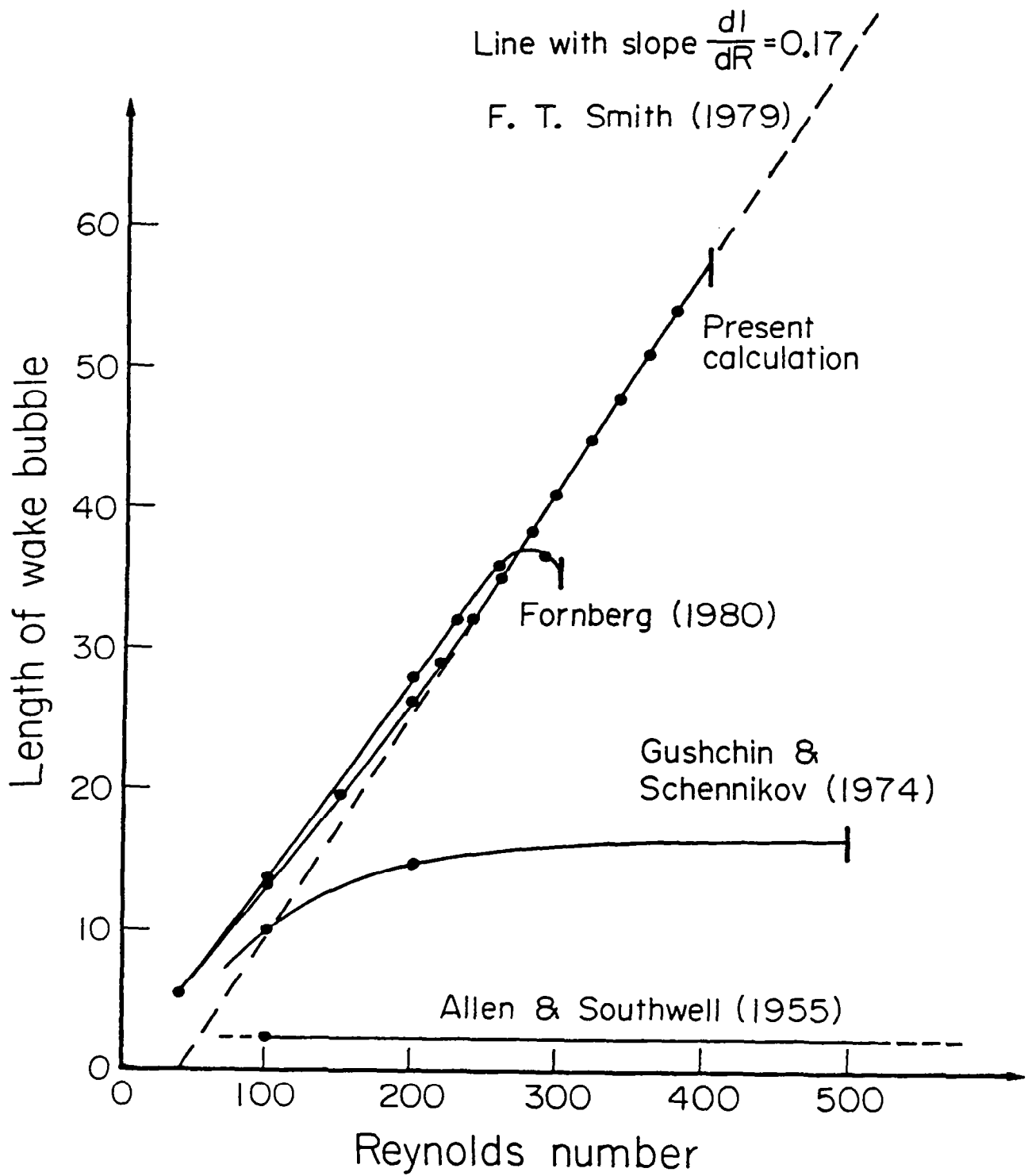218

Figure 8. Modified linear system.

Figure 9: Length of wake bubble for different Reynolds numbers.
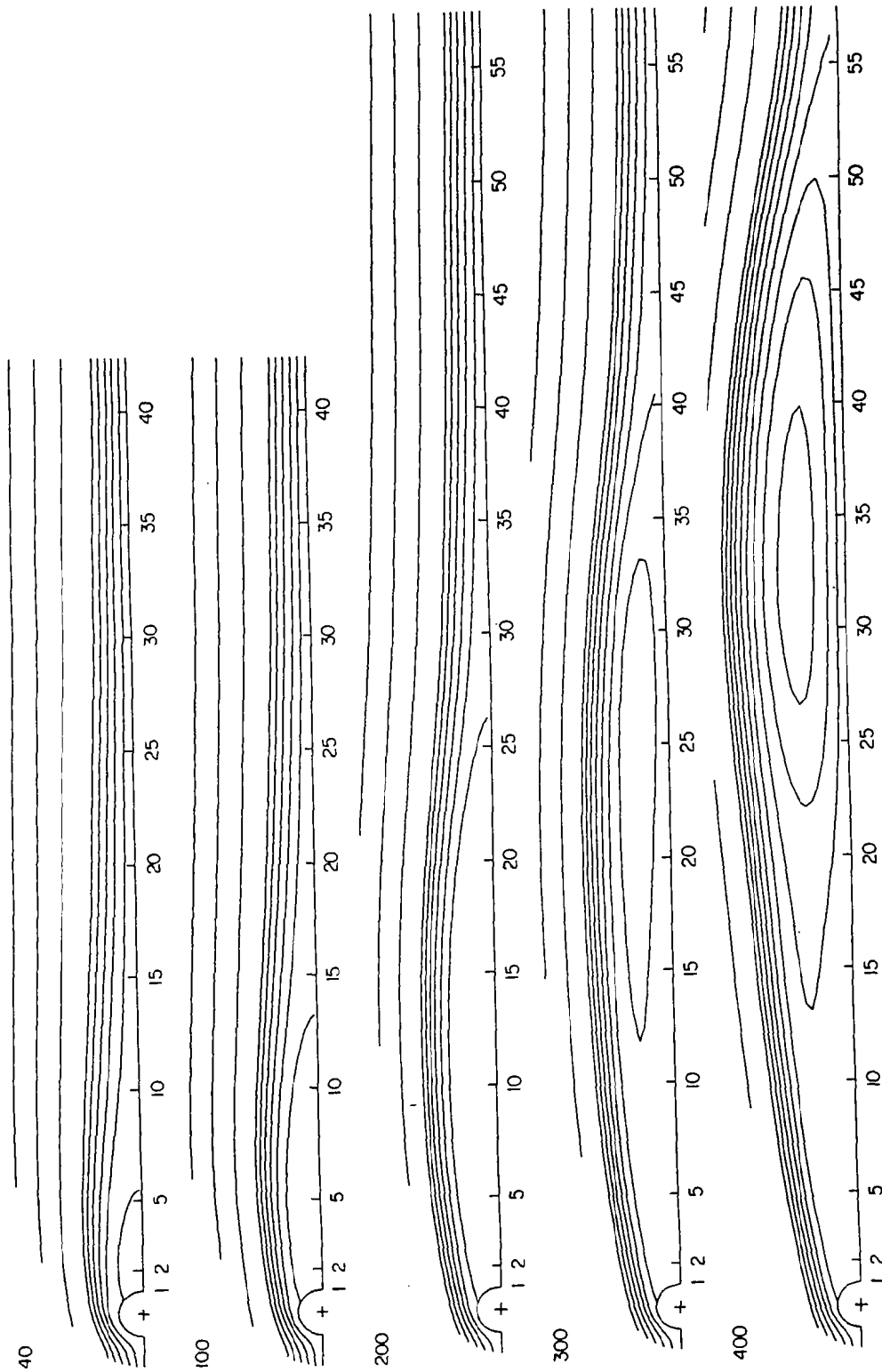
220

Figure 10: Streamlines (values $\psi = -1.4, -1.2, \ldots, .8, 1., 2., \ldots, 8., 9.$) for different Reynolds numbers.

Figure 11: Contours of constant vorticity (values $\omega = -12.$, $-8.$, $-4.$, $-2.$, $-1.$, $-.8$, $-.6$, $-.4$, $-.2$, $-1.$, $0.$, $.1$, $.2$, $.5$) for different Reynolds numbers.

REFERENCES

1. Allen, D.N. de G. & Southwell, R.V.: Relaxation methods applied to determine the motion, in two dimensions, of a viscous fluid past a fixed cylinder. Quart. J. Mech. Appl. Math. 8 (1955) pp 129-145.

2. Batchelor, G.K.: A proposal concerning laminar wakes behind bluff bodies at large Reynolds number. J. Fluid Mech. 1 (1956) pp 388-398.

3. Brodetsky, S.: Discontinuous fluid motion past circular and elliptic cylinders. Proc. Roy. Soc. A 102 (1923) pp 542-553.

4. Dennis, S.C.R.: A numerical method for calculating steady flow past a cylinder. Proc. 5th Int. Conf. on Numerical Methods in Fluid Dynamics (Ed. A.I. van de Vooren & P.J. Zandbergen), Lecture notes in Physics, Springer, vol 59 (1976) pp 165-172.

5. Dennis, S.C.R. & Chang, G.Z.: Numerical solutions for steady flow past a circular cylinder at Reynolds numbers up to 100. J. Fluid Mech. 42 (1970) pp 471-489.

6. Fornberg, B.: A numerical study of steady viscous flow past a circular cylinder, J. Fluid Mech. 98 (1980) pp 819-855.

7. Gushchin, V.A. & Schennikov, V.V.: A numerical method of solving the Navier-Stokes equations. Zh. vychist. Mat. mat. Fiz. (1974), pp 512-520.

8. Imai, I.: On the asymptotic behaviour of viscous fluid flow at a great distance from a cylindrical body, with special reference to Filon's paradox. Proc. Roy. Soc. A 208 pp 487-516.

9. Keller, H.B.: The bordering algorithm and path following near singular points of higher nullity. Submitted to SIAM J. Sci. Stat. Computing.

10. Peregrine, D.H.: Note on the steady high-Reynolds-number flow about a circular cylinder. School of Mathematics, University of Bristol, Report No. AM-81-04 (1981).

11. Roache, P.J.: Computational fluid dynamics. Hermosa Publishers, Albuquerque (1976)

12. Saffman, P.G. & Tanveer, S.: Prandtl-Batchelor flow past a flat plate with a forward facing flap. Manuscript in preparation (1983).

13. Smith, F.T.:Laminar flow of an incompressible fluid past a bluff body: the separation, reattachment, eddy properties and drag. J. Fluid Mech. 92 (1979) pp 171-205.

14. Smith, F.T.: Comparisons and comments concerning recent calculations for flow past a circular cylinder. J. Fluid Mech. 113, pp 407-410.

15. Ta, P.L.: Étude numérique de l'écoulement d'un fluide visqueux incompressible autour d'un cylindre fixe ou en rotation. Effet Magnus. J. Méc. 14 (1975) pp 109-134.

16. Takami,H. & Keller, H.B.: Steady two-dimensional viscous flow of an incompressible fluid past a circular cylinder. Phys. Fluids Suppl. II pp 51-55.